Chemistry & Biology, Vol. 11, 427–437, April, 2004, ©2004 Elsevier Science Ltd. All rights reserved. DOI 10.1016/j.chembiol.2004.03.015

Enhanced Intravenous Transgene Expression in Mouse Lung Using Cyclic-Head Cationic Lipids

Bharat Kumar Majeti,[1,4] Rajkumar Sunil Singh,[1,4] Sudheer Kumar Yadav,[1,5] Surendar Reddy Bathula,[1] Sistla Ramakrishna,[2] Prakash Vamanrao Diwan,[2] Surkara Sakunthala Madhavendra,[3] and Arabinda Chaudhuri[1,*]

[1]Division of Lipid Science and Technology
[2]Pharmacology Division
[3]Electron Microscopy Center
Indian Institute of Chemical Technology
Hyderabad 500 007
India

Summary

Herein, we report enhanced intravenous mouse lung transfection using novel cyclic-head-group analogs of usually open-head cationic transfection lipids. Design and synthesis of the new cyclic-head lipid N,N-di-n-tetradecyl-3,4-dihydroxy-pyrrolidinium chloride (lipid 1) and its higher alkyl-chain analogs (lipids 2–4) and relative in vitro and in vivo gene transfer efficacies of cyclic-head lipids 1–4 to their corresponding open-head analogs [lipid 5, namely N,N-di-n-tetradecyl-N,N-(2-hydroxyethyl)ammonium chloride and its higher alkyl-chain analogs, lipids 6–8] have been described. In stark contrast to comparable in vitro transfection efficacies of both the cyclic- and open-head lipids, lipids 1–4 with cyclic heads were found to be significantly more efficient (by 5- to 11-fold) in transfecting mouse lung than their corresponding open-head analogs (5–8) upon intravenous administration. The cyclic-head lipid 3 with di-stearyl hydrophobic tail was found to be the most promising for future applications.

Introduction

Development of efficacious and safe therapeutic gene carriers is the key to clinical success of gene therapy. Recombinant viral vectors, although capable of ensuring high levels of transgene expression into body cells upon intravenous administration, suffer from numerous disadvantages [1–3]. Adenoviral vectors, for example, generate toxic inflammatory responses [4, 5] and can lead to onset of serious host immune responses against viral structural components [6, 7], thereby preventing their readministration in immunocompetent animals. Additional disadvantages of viral vectors include the following: (1) the possibility of random integration into host chromosome, leading to subsequent activation of proto-oncogenes; (2) systemic clearance of viral vectors due to complement activation; (3) the possibility of generating replication-competent virus through recombination with host genome; (4) the limited insert size of the virally packaged therapeutic genes, etc. [8, 9]. Conversely, cationic lipids, because of their less immunogenic nature, robust manufacture, ability to deliver very large pieces of DNA, and ease in handling and preparation techniques, are increasingly becoming the alternative nonviral vectors of choice in gene therapy [10–21].

Lung is one of the most intensely studied sites for pharmaceutical intervention in gene therapy. Cystic fibrosis (CF), for example, is a monogenic inherited disorder caused by any of over 1000 mutations in a 230 kb gene on chromosome 7 encoding a 1480 amino acid polypeptide, named cystic fibrosis transmembrane conductance regulator (CFTR), that functions as a chloride ion channel in lung epithelial cell membranes [22].

Lung epithelial cells possessing mutant CFTR genes are incapable of expressing the functional CFTR proteins, which in turn leads to pathogenic ion transport defects in lungs. Gene expression and appropriate physiological effects have been observed following cationic lipid-mediated administration of wild-type CFTR cDNA into the lung epithelial cells of transgenic CF mice [23, 24] and human CF patients [25]. The focus of many subsequently reported strategies for nonviral systemic lung transfection have been centered around the use of either novel cationic lipids or improved formulations of known cationic amphiphiles and DNA [10, 11, 15]. The latest investigations have demonstrated the enormous therapeutic potential of using lung as a genetic metabolic factory to produce and deliver proteins into the circulation for treatment of inherited diseases not directly associated with lung pathology [26]. Taken together, ensuring clinical success of cationic liposomes in nonviral gene therapy for treatment of lung-related inherited diseases will remain critically dependent on the use of cationic lipids efficient in delivering genes of interest into lung cells.

We have recently reported on design, synthesis, and high in vitro transfection efficacies of a number of open-head non-glycerol-based cationic lipids containing hydrogen bonding hydroxyl head groups for use in nonviral gene delivery [19–21, 27]. With a view to probe the relative transfection efficacies of such open-head hydroxyl group containing cationic lipids with their cyclic-head counterparts, we designed and synthesized four novel cyclic-head cationic lipid analogs (**1–4**, Figure 1) of our previously reported [27] open-head lipids **5–8** (Figure 1). Surprisingly, in sharp contrast to their comparable in vitro gene transfer properties, in vivo experiments revealed remarkably superior lung transfection efficacies of this new generation of cyclic-head cationic lipids (**1–4**) compared to their open-head courterparts (**5–8**). Herein, we delineate the first examples of enhanced intravenous gene expression in mouse lung using cyclic head-group analogs of usually open-head cationic transfection lipids.

Results and Discussion

Chemistry

Lipids **1–4** (Figure 1A), the cyclic head-group analogs of our recently developed [27] open-head cationic trans-

*Correspondence: arabinda@iict.res.in

[4]These authors contributed equally to this work.

[5]This work is dedicated to the memory of the recently expired Sudheer Kumar Yadav, a creative young doctoral student whose dream was to become a chemical biologist.

A Synthesis of Cyclic-Headgroup analogs:

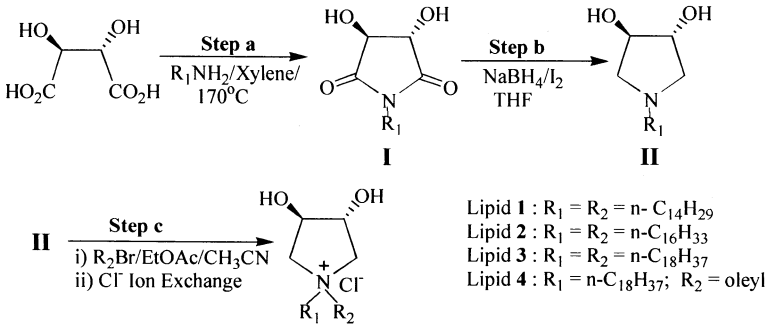

Lipid **1** : $R_1 = R_2 =$ n- $C_{14}H_{29}$
Lipid **2** : $R_1 = R_2 =$ n-$C_{16}H_{33}$
Lipid **3** : $R_1 = R_2 =$ n-$C_{18}H_{37}$
Lipid **4** : $R_1 =$ n-$C_{18}H_{37}$; $R_2 =$ oleyl

B Structures of Open-Headgroup analogs:

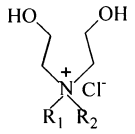

Lipid **5** : $R_1 = R_2 =$ n-$C_{14}H_{29}$
Lipid **6** : $R_1 = R_2 =$ n-$C_{16}H_{33}$
Lipid **7** : $R_1 = R_2 =$ n-$C_{18}H_{37}$
Lipid **8** : $R_1 =$ n- $C_{18}H_{37}$; $R_2 =$ oleyl

Figure 1. Syntheses and Structures of the Cyclic- and Open-Head Cationic Lipids

(A) Synthesis of cyclic-head cationic lipids **1–4**.

(B) Chemical structures of cationic lipids **5–8**.

fection lipids **5–8** (Figure 1B), were designed to decode the relative in vitro and in vivo transfection efficacies of cationic lipids with open and cyclic polar heads. In terms of bond connectivity patterns, the only difference between the molecular structures of cyclic-head lipids **1–4** and their open-head analogs lipids **5–8** is that the hydroxyl-group-bearing carbon atoms are covalently linked to each other in lipids **1–4**, and in lipids **5–8** they are not. Lipids **1–4** were synthesized by dehydrative coupling [28] of the appropriate hydrophobic primary amine to L(+)-tartaric acid (Figure 1A) in refluxing xylene so that water formed during the reaction could be separated by azeotropic distillation in a Dean-Stark apparatus. The resulting N-n-alkyl-3,4-dihydroxy-2,5-dioxo pyrrolidine (cyclic imide interemedite **I**, Figure 1A), upon reduction with sodium borohydride/iodine, afforded the corresponding tertiary amine intermediate **II** (Figure 1A), the immediate precursor of the target lipids. Intermediate **II**, upon quaternization with hydrophobic alkyl bromide in 3:1 (v/v) ethylacetate/acetonitrile followed by chloride ion exchange on Amberlyst-A26 resin, afforded the target lipids with cyclic 3,4-dihydroxy-pyrrolidinium head groups (lipids **1–4**, Figure 1A).

In Vitro Transfection Studies

Before beginning our in vivo experiments, we first evaluated the in vitro transfection efficacies of both cyclic-head (**1–4**) and open-head (**5–8**) lipids against three cultured mammalian cells, COS-1, CHO, and HepG2, across the lipid:DNA charge ratios 9:1–0.1:1 (Figures 2A–2C) using pCMV-SPORT-β-gal plasmid as the reporter gene. Consistent with many other previously reported in vitro studies, both the open-head and cyclic-head lipids were found to be optimally efficient around lipid:DNA charge ratio (+/−) of 1:1 (Figures 2A–2C) using cholesterol as a colipid at lipid:colipid mole ratio of 1:1 (contrary to many other reports, the usual colipid DOPE was found to abolish the transfection efficacies of present open- and cyclic-head lipids; data not shown). Both cyclic- and open-head lipids with di-myristyl (**1** and **5**) and di-palmityl (**2** and **6**) tails were found to be slightly more efficient than lipids with di-stearyl (**3** and **7**) and oleyl-stearyl (**4** and **8**) anchors in transfecting CHO and HepG2 cells (Figures 2B and 2C). In COS-1 cells, however, except the lipids with oleyl-stearyl tails (**4** and **8**), all the other lipids with both cyclic and open heads were found to be remarkably transfection efficient (Figure 2A). Interestingly, at 1:1 lipid:DNA charge ratio, no statistically significant difference in in vitro transfection properties were observed for the corresponding open-head and cyclic-head lipids with same hydrophobic tails, such as lipids **1** and **5**, **2** and **6**, **3** and **7**, etc. (Figures 2A–2C). In other words, the in vitro transfection efficacies of cyclic- and open-head lipids with the same anchor lengths were observed to be similar. The in vitro transfection efficiencies of many of the present open- and cyclic-head lipids (particularly those with myristyl and palmityl chains) were observed to be better than or comparable to that of **1**, 2-dimyristyloxypropyl-3-dimethyl-hydroxyethyl ammonium bromide (DMRIE-C), one of the most popular commercially available cationic transfection lipids, containing a 2-hydroxyethyl functionality directly attached to the quaternized nitrogen atom (Figures 2A–2C). Interestingly, both the cyclic- and open-head lipids **4** and **8**, in spite of having membrane-reorganizing unsaturated oleyl chains, showed reduced transfection efficacies in all three cells (Figures 2A–C). Taken together, the in vitro transfection efficacies of both cyclic and open-head lipids were found to be equally impressive.

In Vivo Transfection Studies

Initial experiments across the lipid:DNA (+/−) charge ratios of 2:1–15:1 revealed 4:1 as the optimal in vivo

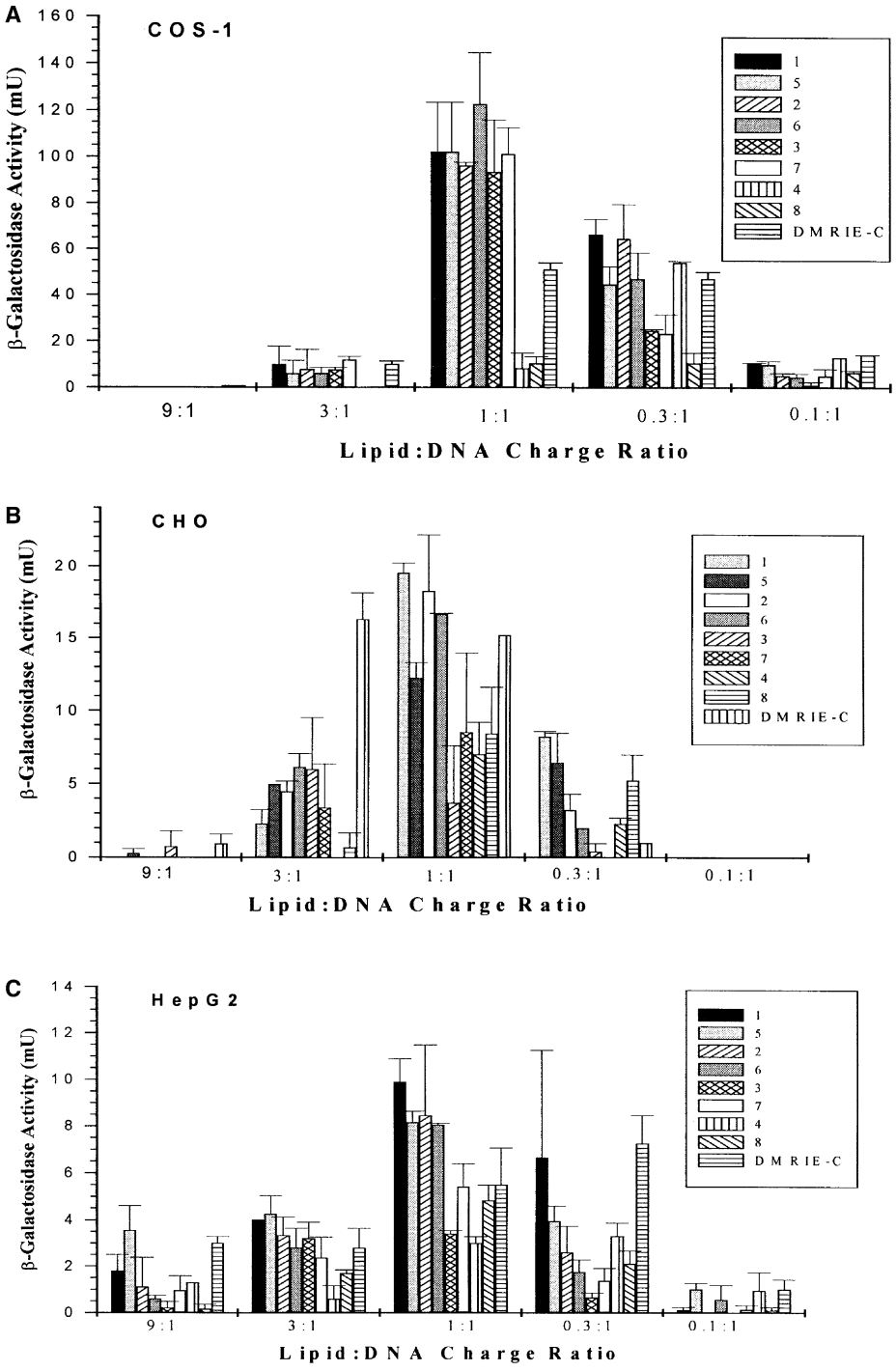

Figure 2. Relative In Vitro Transfection Profiles of the Cyclic- and Open-Head Cationic Lipids

In vitro transfection efficiencies of lipids **1–8** in COS-1 (A), CHO (B), and HepG2 cells (C) using cholesterol as colipid (at 1:1 molar ratio of lipid:cholesterol). The transfection efficiencies of the lipids were compared to that of the commercially available reagent DMRIE-C. The β-galactosidase activities in each well were converted to absolute β-galactosidase milli-units using a standard curve constructed with pure (commercial) β-galactosidase. All of the lipids were tested on the same day, and the data presented are the average value of two replicate experiments performed on the same day.

charge ratio for the present lipids (data not shown). Preliminary time-course studies showed that onset of gene expression by the present lipids started at 6 hr post-injection, with the strength of transgene expressions remaining at maximum values during 8–24 hr post-injection and then decreasing gradually within 48 hr (data not shown). Thus, in all subsequent in vivo experiments, transgene expressions were routinely monitored

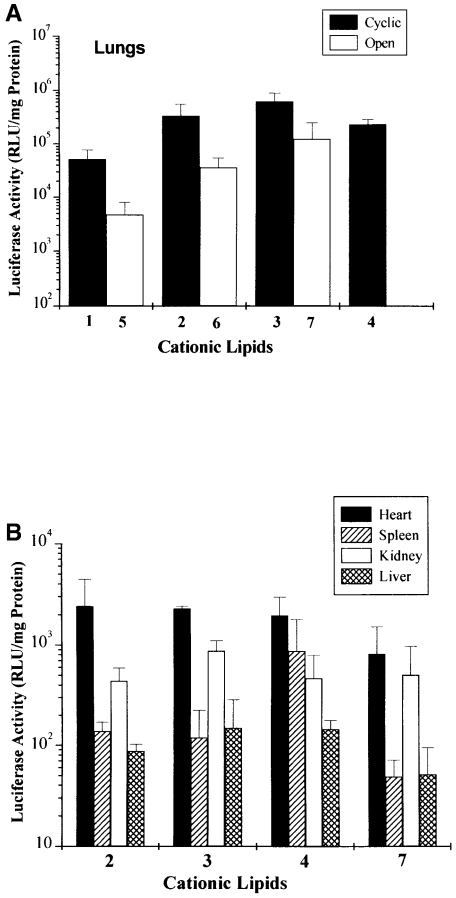

Figure 3. Relative In Vivo Transfection Profiles of the Cyclic- and Open-Head Cationic Lipids

(A) Comparative transfection efficiencies of cyclic- and open-head cationic lipids **1–7** in mouse lung.

(B) Comparative transfection efficiencies of cationic lipids **2**, **3**, **4**, and **7** in heart, spleen, kidney, and liver. Each mouse was intravenously injected with 25 μg of pCMV-Luc complexed to different cationic lipids at lipid:DNA molar ratio of 4:1. Luciferase activity was estimated 8 hr post-injection, as described in the text. Data shown are the mean ±SD (n = 3).

8 hr post-injection. As observed in many other in vivo gene transfer studies, remarkable transgene expressions were primarily observed in mice lungs (Figure 3A). Heart was found to be transfected by lipids **2**, **3**, **4**, and **7** with about 250- to 300-fold less efficiency than lung transfection by lipid **3**, while expressions in other organs like kidney, spleen, and liver progressively diminished (Figure 3B).

Several contrasting features of open- and cyclic-head lipids were observed. Although open- and cyclic-head cationic lipids with myristyl, palmityl, and stearyl tails showed nearly comparable in vitro transfection efficacies (Figures 2A–2C), the efficacies of intravenous lung transfections were found to increase with increasing tail hydrophobicities of both open- and cyclic-head lipids (Figure 3A). In stark contrast to comparable in vitro transfection efficacies of cyclic- and open-head lipids with the same hydrocarbon tails (Figures 2A–2C), lipoplexes of lipids **1–4** (complexes of lipids and pCMV-luc at lipid:DNA charge ratio of 4:1) were found to be 5- to 11-fold more efficient in transfecting mouse lung than their corresponding open-head analogs **5–8** upon intravenous administration (Figure 3A); lipid **3** with di-stearyl hydrophobic tail being the most promising one for future applications. Toward further improving efficacies of lipid **3**, we tried a reported method of precondensing reporter gene with protamine sulfate [29, 30]. Unfortunately, such a strategy did not enhance lung transfection efficiency of lipid **3** (data not shown). An important observation deserves to be mentioned at this point: although the cyclic-head lipid **4** with oleyl-stearyl tail showed significant lung transfection efficacy (Figure 3A), half of the animals injected died within 8 hr post-injection. The picture became worse with lipid **8** (the open-head analog of lipid **4**): animals died within 2 hr of injecting lipoplexes of lipid **8** (hence, the open bar data for lipid **8** are missing in Figure 3A).

Plasma is thought to be one of the major barriers impeding the efficiencies of intravenous gene delivery mediated by cationic lipoplexes [31–33]. Investigations aimed at understanding the interaction of various plasma components with cationic lipoplexes have just begun [34]. Identifications of various plasma proteins capable of binding with lipid:DNA complexes and thereby destroying their in vivo transfection efficacies are yet to be deciphered. Thus, the origin of the observed enhanced lung transfection by cyclic-head lipids (**1–4**) compared to their open-head analogs is an open question at the present state of investigation. Clearly, preclinical formulation parameters need to be optimized further before evaluating the clinical potentials of the presently described cyclic-head cationic lipids for transfecting lungs of human CF patients with CFTR gene. For instance, at the current stage of investigation, the present lipids show transient gene expression. Investigations aimed at accomplishing long-term expression using better lipid formulations and improved expression plasmids are currently in progress in our laboratories.

Physicochemical Characterizations of Liposomes and Lipoplexes

Lipoplex Sizes and Zeta Potentials

Measurements of particle sizes using the dynamic laser light scattering technique revealed that the sizes of tail-vein-injected lipoplexes with lipid:DNA charge ratios of 4:1 prepared in 5% glucose solution are sensitive to the ionic strength of the medium. The sizes increased from around 100 nm in the absence of any added salt to 150–200 nm (by a factor of 1.5–2.0) in the presence of 150 mM sodium chloride (Table 1); except in case of lipid **4**, where the corresponding size increase was almost 3-fold (from 104 nm to 273 nm; Table 1A). This range is well within the size range of many previously reported in vivo-efficient lipoplexes and is consistent with high DNA-compacting properties of the present lipids (given that naked plasmid DNA are usually bigger than 400 nm). The larger lipoplexes, in the presence of DMEM at 1:1 lipid:DNA charge ratio (with sizes mostly in the range of 210–250 nm; Table 1A), are more representative of the particle sizes involved in the in vitro experiments. Figure 4 shows the morphological charac-

Table 1. Size and Surface-Charge Characteristics of the Open- and Cyclic-Head Liposomes and Lipoplexes

A. Hydrodynamic Diameters and Zeta Potentials of Liposomes and Lipoplexes

Lipids	Hydrodynamic Diameter (nm)				Zeta Potential (mV)		
	Lipid:DNA (1:0) H_2O	Lipid:DNA (1:1) (DMEM)	Lipid:DNA (4:1) (5% glucose)	Lipid:DNA (4:1) (5% glucose + 0.15M NaCl)	Lipid:DNA (1:1) (DMEM)	Lipid:DNA (4:1) (5% glucose)	Lipid:DNA (4:1) (5% glucose + 0.15M NaCl)
1	122 ± 1	213 ± 6	107 ± 2	179 ± 1	−36 ± 2	19 ± 3	38 ± 1
5	121 ± 9	218 ± 2	102 ± 2	156 ± 1	−37 ± 1	21 ± 3	34 ± 2
2	111 ± 2	227 ± 5	126 ± 2	196 ± 3	−49 ± 3	17 ± 4	41 ± 1
6	123 ± 3	221 ± 2	104 ± 2	158 ± 2	−36 ± 3	23 ± 3	38 ± 2
3	138 ± 3	239 ± 1	116 ± 2	217 ± 10	−37 ± 1	21 ± 3	39 ± 4
7	143 ± 3	252 ± 4	108 ± 4	189 ± 6	−33 ± 2	18 ± 3	37 ± 3
4	118 ± 3	172 ± 1	105 ± 4	273 ± 5	−33 ± 1	17 ± 2	39 ± 2
8	107 ± 2	245 ± 1	95 ± 1	191 ± 4	−38 ± 2	19 ± 3	34 ± 2

B. Hydrodynamic Diameters and Zeta Potentials (ζ) of Lipoplexes in the Presence of 90% Mouse Serum

Time (min)	Hydrodynamic Diameter (nm)		Zeta Potential (mV)	
	Lipid **3**:DNA (4:1)	Lipid **7**:DNA (4:1)	Lipid **3**:DNA (4:1)	Lipid **7**:DNA (4:1)
15	109 ± 4	133 ± 5	−8 ± 2	−9 ± 1
30	108 ± 2	126 ± 1	−10 ± 2	−12 ± 1
60	115 ± 1	134 ± 3	−12 ± 2	−8 ± 1
90	120 ± 2	138 ± 1	−11 ± 3	−8 ± 1
120	130 ± 5	147 ± 2	−11 ± 3	−9 ± 2

Average sizes and zeta potentials were measured by a laser light scattering technique using Zetasizer 3000A (Malvern Instruments, United Kingdom). Values of the hydrodynamic diameters shown are the average of three independent size measurements (calculated by the instrument-specific cumulant analysis software), where each measurement is the average size of 10 submeasurements. Typical poly-dispersity indices for liposomes and lipoplexes in the presence of 5% glucose, 5% glucose + 0.15M NaCl, and DMEM varied from 0.10 to 0.35, while those in the presence of mouse serum varied from 0.50 to 0.60. The zeta potential values shown are the average of 10 independent surface potential measurements.

teristics of the representative lipoplexes **3** and **7** (prepared with lipid:DNA charge ratio of 4:1 in deionized water) obtained by using transmission electron microscopy. Particle sizes obtained from transmission electron microscopy (Figure 4) were consistent with those obtained using the dynamic laser light scattering technique (Table 1A). Interestingly, transmission electron microscopic pictures revealed a closely associated network of lipoplexes only for those prepared with open-head lipid **7** and not for lipoplexes prepared using the cyclic-head lipid **3**. However, whether or not such networking tendencies of lipoplex **7** have any correlation with its poor lung transfection efficacies remains elusive at this point.

Interestingly, global surface potentials (zeta potentials, measured by a dynamic light scattering instrument with zeta-sizing capacity) of almost all of the present lipoplexes used in the in vitro experiments were similarly negative in the presence of DMEM (Table 1A). Surface charges of previously reported efficient cationic lipoplexes prepared using lipid:DNA charge ratios of 1:1 have been shown to be similarly negative in the presence of DMEM [35]. This observation supports the notion that global surface charges are unlikely to play any major role in modulating in vitro transfection efficacies of cationic lipids. The surface potentials of all the tail-vein-injected lipoplexes prepared using 4:1 lipid:DNA charge ratio in 5% glucose solutions were observed to be close to +20 mV and increased almost by a factor of two in the presence of 150 mM sodium chloride (Table 1A). Such a high positively charged character of the present lipoplexes is likely to prevent rapid DNA dissociation from lipoplexes while in circulation.

Serum Stabilities

With a view to assess the stability profiles of the present lipoplexes under the physiological concentration range of mouse serum, both size and global surface potentials of lipoplexes **3** and **7** (as representative examples) in the presence of 90% freshly collected mouse serum were determined using a dynamic laser light scattering technique across a range of incubation times (15–120 min) at 37°C. The global surface potential measurements (using a dynamic laser light scattering instrument equipped with zeta-sizing capacity) for lipoplexes **3** and **7** with 4:1 lipid:DNA charge ratios across this incubation time range revealed the existence of similar negative surface charges for both in the presence of 90% mouse serum (−8.0 mV to −12.0 mV; Table 1B). These results are consistent with negatively charged lipoplex particles being involved in the present in vivo lipofection.

Up to 2 hr of incubation in the presence of 90% mouse serum, particle sizes of both the lipoplexes were well within the usual size ranges for intravenous applications, with the sizes of the open-head lipoplexes **7** remaining somewhat higher (126–147 nm) than those of its cyclic-head counterpart **3** (108–130 nm; Table 1B). However, after 2.5 hr incubation in the presence of 90% mouse serum, the entire mixture within the cuvette transformed to a gel-like material for both the lipoplexes **3** and **7**, and no size measurements were possible beyond this time point. Interestingly, much faster aggregation (within 15–90 min) was observed when lipoplexes **3** and **7** were

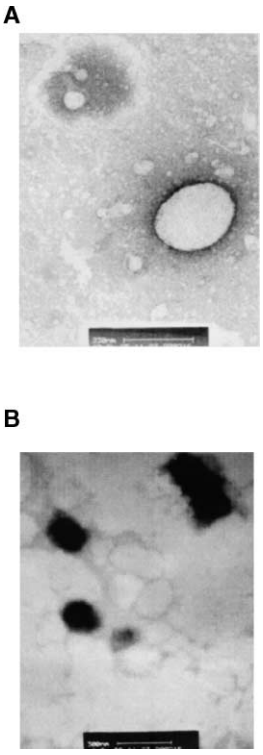

Figure 4. Transmission Electron Micrographs of Representative Lipoplexes

Transmission electron micrographs of lipid:DNA complexes prepared from lipid **3** (A) and lipid **7** (B) and pCMV-Luc at lipid:DNA charge ratio of 4:1. Bars correspond to 230 nm.(A) and 330 nm (B).

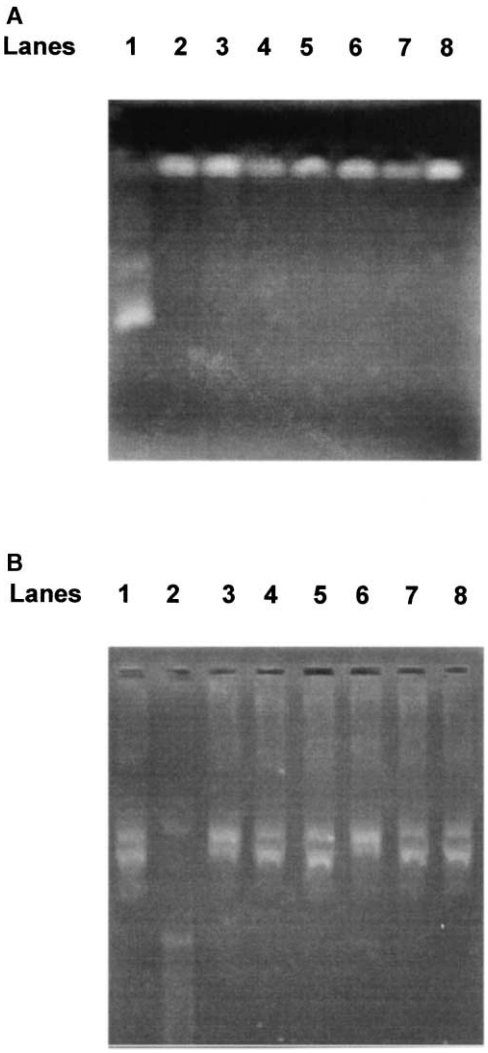

Figure 5. Results of the Gel Retardation and DNase-I Sensitivity Assays

(A) Electrophoretic mobilities of the lipid-DNA complexes made from lipids **1–7** and pCMV-Luc (at lipid:DNA charge ratio of 4:1) through a 1% agarose gel. Free pCMV-Luc was loaded in lane **1**, and lanes 2, 3, 4, 5, 6, 7, and 8 were used for loading lipoplexes of cationic lipids **1**, **2**, **3**, **4**, **5**, **6**, and **7**, respectively.

(B) DNase I sensitivities of lipid-DNA complexes made from lipids **3** and **7** and pCMV-Luc. Free pCMV-Luc and pCMV-Luc treated with DNase I were loaded in lanes 1 and 2. DNase I treated lipoplexes of lipid **7** at lipid:DNA charge ratios of 1:1, 4:1, and 9:1 were loaded in lanes 3, 4, and 5, respectively. Similarly, DNase I-treated lipoplexes of lipid **3** at lipid:DNA charge ratios of 1:1, 4:1, and 9:1 were loaded in lanes 6, 7, and 8.

incubated with 10%–70% mouse serum (data not shown). Such serum-induced rapid aggregation of lipoplexes have been reported previously by Li et al., who demonstrated that the balance between the initial aggregation rates in the lung capillaries and the rates of the subsequent disintegration of lipidic vectors by serum dictates their lung lipofection efficacies [33]. Similar aggregation behaviors of the lipoplexes prepared from lipids **3** and **7** in the presence of varying serum concentrations indicate that both the lipoplexes are likely to be efficiently entrapped in the lung capillaries (thereby showing enhanced lung transfection). Thus, based on the findings of Li et al. [33], the remarkably higher lung transfection efficiency of lipid **3** may possibly be related to its higher subsequent serum-induced disintegration rate compared to that for lipid **7**. Clearly, detailed ultrastructural investigations after exposing the lipoplexes to varying mouse serum concentrations for different incubation periods and particle distribution studies using radiolabeled lipoplexes will be needed to gain mechanistic insights into the origin of the remarkably higher lung transfection properties of lipid **3** than of lipid **7**.

Lipid:DNA Binding Interactions and Lipoplex Sensitivities to DNase I

With a view toward gaining insights into the role of lipid:DNA electrostatic binding interactions in modulating the in vivo transfection efficacies of the present lipids, conventional gel retardation assays were performed using lipoplexes prepared with the optimum in vivo lipid:DNA charge ratios of 4:1. Results of such gel retardation assays (Figure 5A) provided convincing support for the existence of strong electrostatic interactions between lipids **1–7** and plasmid DNA at 4:1 lipid:DNA charge ratio (lipid **8** was skipped because it was observed to be toxic, as described below). Such remarkable lipid:DNA electrostatic binding interactions observed in conventional gel retardation assay (Figure 5A) were further confirmed by monitoring the sensitivities

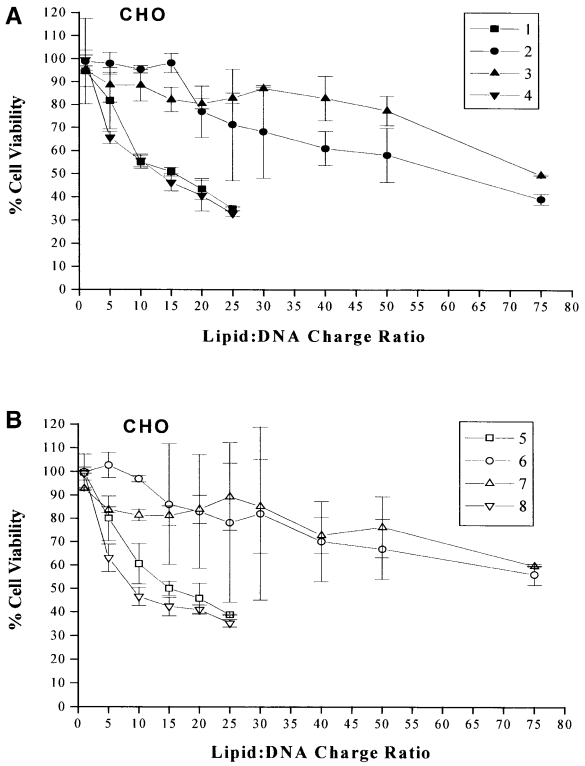

Figure 6. Cell Viabilities of the Cyclic- and Open-Head Cationic Lipids

MTT-assay-based cell viabilities of lipids **1–4** (A) and **5–8** (B) in CHO cells (details are described in the main text). The data presented are average values of duplicate experiments (n = 2). Results were expressed as percent viability = [A_{550}(treated cells)-background]/[A_{550}(untreated cells)-background] × 100.

of the representative lipoplexes **3** and **7** upon treatment with DNase I at lipid:DNA charge ratios of 9:1, 4:1, and 1:1. After the free DNA digestion by DNase I, the total DNA (both the digested and inaccessible DNA) were separated from lipid (by extracting with organic solvents) and loaded on a 1% agarose gel. Consistent with observations in the gel retardation assays (Figure 5A), DNase I digestion assays (Figure 5B) did not reveal the existence of any significant electrostatic interaction difference between lipoplexes prepared from the representative cyclic-head and open-head cationic lipids **3** and **7**. Taken together, the results summarized in Figure 5 support the notion that electrostatic lipid:DNA interactions are unlikely to be significantly different for both the presently described open-head and cyclic-head lipids.

Cell Viabilities

To assess the relative cytotoxicities and IC_{50} concentrations of the present cationic lipids, cell viabilities of lipoplexes **1–8** were measured using MTT-based cell viability assays in representative CHO cells across a wide range of lipid:DNA charge ratios of 1:1–75:1. Interestingly, cell viability profiles of the cyclic-head lipoplexes **1–4** across this entire range of lipid:DNA charge ratios (Figure 6A) were found to be remarkably similar to those for the corresponding open-head lipoplexes **5–8** (Figure 6B). Except the lipids containing oleyl and stearyl chains (**4** and **8**), all of the remaining lipoplexes prepared from both the cyclic- and open-head lipids showed more than 80% cell viabilities up to lipid:DNA charge ratios of 4:1 (Figure 6). However, the tendency of percent cell viabilities to decrease with increasing lipid:DNA charge ratios was found to be significantly more pronounced for lipids with di-myristyl and oleyl-stearyl anchors for both the open-head and cyclic-head series, compared to their di-palmityl and di-stearyl counterparts (Figure 6). The IC_{50} (inhibitory concentrations of lipids required to inhibit cell viabilities by 50%) values for lipids **1–8** were directly estimated (from Figure 6) to be about 75, 285, 340, 60, 70, >340, >340, and 40 μM, respectively. Thus, the observed poor transfection efficacies of lipids **4** and **8** (Figure 2) correlate well with their relatively high in vitro cellular toxicities and low IC_{50} values. Conversely, the relatively high IC_{50} values (≥340 μM) for lipids **3**, **6**, and **7** certainly make these lipids worthy of exploiting in future in vivo applications.

Significance

Designing safe and efficient nonviral transfection vectors for use in gene therapy is an intensely pursued area of research at the interface of chemistry and biology. Cationic lipids, because of their least immunogenic nature, are increasingly becoming the nonviral vectors of choice in effecting in vivo transgene expression. A vast majority of the existing cationic transfection lipids contain conformationally unstrained polar functional groups in their head-group regions. In order to probe the relative transfection efficacies of usually open-head cationic lipids and their conformationally strained cyclic-head counterparts, we have designed and synthesized four novel cyclic-head analogs of previously reported open-head cationic transfection lipids with tails of increasing hydrophobicity and evaluated their transfection efficiencies (both in vitro and in vivo). Herein, we demonstrate that in vivo lung transfection efficacies of cationic lipids can be significantly (5- to 11-fold) enhanced through design and synthesis of appropriate conformationally strained cyclic-head analogs of their usually open-head structures. Similar aggregation behavior of lipoplexes 3 and 7 in the presence of varying serum concentrations indirectly supports the notion that both of the lipoplexes are efficiently entrapped in the lung capillaries. The superior lung transfection efficiency of the cyclic-head lipid might possibly be related to its faster subsequent serum-induced distintegration rate compared to that for lipid 7. The present findings are likely to provide impetus for future structure-activity investigations aimed at improving in vivo transfection properties of usually open-head cationic transfection lipids through designing their appropriate cyclic-head analogs.

Experimental Procedures

General Procedures and Reagents

The FABMS analyses were performed on a Micromass AUTOSPEC-M mass spectrometer (Manchester, United Kingdom) with OPUS V3, 1X data system. Data were acquired by liquid secondary ion mass spectrometry (LSIMS) using *meta*-nitrobenzyl alcohol as the matrix. ^{1}H NMR spectra were recorded on a Varian FT 200 MHz. 1-bromotetradecane, 1-bromohexadecane, 1-bromooctadecane,

n-tetradecylamine, n-hexadecylamine, and n-octadecylamine were procured from Lancaster (Morecambe, United Kingdom). Column chromatography was performed with silica gel (Acme Synthetic Chemicals, India, 60–120 mesh). DMRIE-C reagent was purchased from Gibco BRL, Life Technologies. Cell culture media, fetal bovine serum, 3-(4,5-dimethylthiazol-2-yl)-2,5-diphenyltetrazolium bromide (MTT), polyethylene glycol 8000, *o*-nitrophenyl-β−D-galactopyranoside, and cholesterol were purchased from Sigma, St. Louis, MO. NP-40, antibiotics, and agarose were purchased from Hi-Media, India. Unless otherwise stated, all other reagents purchased from local commercial suppliers were of analytical grades and were used without further purification.

Synthesis of Lipids 1–4

Lipids **1–4** were synthesized following strategies depicted schematically in Figure 1A. As a representative experimental detail, synthesis of only lipid **1** is outlined below. Lipids **2–4** were synthesized following the same protocol as described for lipid **1**. ^{1}H NMR and mass spectral data of all of the purified new cationic lipids **1–4** with cyclic head groups are provided below the synthetic details for lipid **1**. The cyclic tertiary amine intermediate **II** (Figure 1A) was prepared from L(+)-tartaric acid essentially following a procedure described previously [28]. The open-head cationic lipids **5–8** (Figure 1B) were synthesized as described previously [27].

Synthesis of Lipid 1

Step A

Synthesis of N-tetradecyl-3,4-di-hydroxy-2,5-dioxo-pyrrolidine (I, R_1 = n-$C_{14}H_{29}$, Figure 1A). In a 500 ml round-bottomed flask, n-tetradecylamine (21.3 g, 100 mmol) was refluxed in xylene (200 ml) with L(+)-tartaric acid (15 g, 100 mmol) for 3 hr. The water formed in the reaction was removed azeotropically using a Dean-Stark apparatus. After completion of water removal in the Dean-Stark, the reaction mixture was cooled, and the crystalline product was filtered off and washed with hexane (100 ml). The crude product upon recrystallization from hexane-methanol (4:1, 100 ml) afforded 15.2 g (47% yield) of the pure N-tetradecyl-3,4-dihydroxy-2,5-dioxo pyrrolidine as a white solid (R_f = 0.5, 10% methanol/ chloroform, v/v).

N-n-tetradecyl-3,4-dihydroxy-2,5-dioxo pyrrolidine (I, R_1 = n-$C_{14}H_{29}$, Figure 1A). ^{1}H NMR (200 MHz, $CDCl_3$ + DMSO-d_6): δ/ppm = 0.90 [t, 3H, $C\underline{H}_3$-$(CH_2)_{13}$-], 1.20-1.40 [bs, 22H, -$(C\underline{H}_2)_{11}$-], 1.50-1.85 [m, 2H, N(-CH_2-$C\underline{H}_2$-)], 3.30-3.50 [t, 2H, N-$C\underline{H}_2$-$(CH_2)_{12}$-], 4.30-4.40 [bs, 2H, -C<u>H</u>(OH)-C<u>H</u>(OH)-], 6.00-6.20 [bs, 2H, -O<u>H</u>].

N-n-hexadecyl-3,4-dihydroxy-2,5-dioxo pyrrolidine (I, R_1 = n-$C_{16}H_{33}$, Figure 1A). ^{1}H NMR (200 MHz, $CDCl_3$ + DMSO-d_6): δ/ppm = 0.90 [t, 3H, $C\underline{H}_3$-$(CH_2)_{15}$-], 1.10-1.30 [bs, 26H, -$(C\underline{H}_2)_{13}$-], 1.40-1.60 [m, 2H, N(-CH_2-$C\underline{H}_2$-)], 3.30-3.40 [t, 2H, N-$C\underline{H}_2$-$(CH_2)_{14}$-], 4.20-4.30 [bs, 2H, -C<u>H</u>(OH)-C<u>H</u>(OH)-], 6.00-6.20 [bs, 2H, -O<u>H</u>].

N-n-octadecyl-3,4-dihydroxy-2,5-dioxo pyrrolidine (I, R_1 = n-$C_{18}H_{37}$, Figure 1A). ^{1}H NMR (200 MHz, $CDCl_3$ + DMSO-d_6): δ/ppm = 0.90 [t, 3H, $C\underline{H}_3$-$(CH_2)_{17}$-], 1.10-1.40 [bs, 30H, -$(C\underline{H}_2)_{15}$-], 1.50-1.65 [m, 2H, N(-CH_2-$C\underline{H}_2$-)], 3.30-3.50 [t, 2H, N-$C\underline{H}_2$-$(CH_2)_{16}$-], 4.30-4.40 [bs, 2H, -C<u>H</u>(OH)-C<u>H</u>(OH)-], 6.00-6.20 [bs, 2H, -O<u>H</u>].

Step B

Synthesis of N-n-tetradecyl-3,4-dihydroxypyrrolidine (II, R_1 = n-$C_{14}H_{29}$, Figure 1A). N-n-tetradecyl-3,4-dihydroxy-2,5-dioxo pyrrolidine, **I** (7.0 g, 21 mmoles, prepared in Step A above) dissolved in dry tetrahydrofuran (50 ml) was added to a stirred slurry of $NaBH_4$ (4.40 g, 116 mmoles) in tetrahydrofuran (50 ml) in a 500 ml two-necked round-bottomed flask equipped with a reflux condenser and a dropping funnel. Iodine (13.04 g, 51 mmoles) dissolved in tetrahydrofuran (100 ml) was added from the dropping funnel under N_2 atmosphere at 0°C for a period of 2.5 hr. The mixture was refluxed for 6 hr, cooled to 0°C, and the excess sodium borohydride was carefully decomposed with 3N HCl (10 ml). After the evolution of gas ceased, the mixture was neutralized with 3N NaOH (15 ml), the organic layer was separated, and the aqueous layer was extracted with ether (150 ml). The combined organic extract was washed with brine (100 ml), water (2 × 100 ml), and dried over anhydrous Na_2SO_4. After evaporating the solvent on a rotary evaporator, the crude product was dissolved in 30 ml methanol, and 6 ml 12N HCl was added to it. After the exothermic reaction, methanol was distilled off and the mixture was diluted with methanol (50 ml), which was removed again. This process was repeated three times. The residue obtained was treated with a solution of potassium hydroxide (1 g) in methanol (25 ml), and solid anhydrous potassium carbonate (35 g) was added. The solution was filtered and the solvent from filtrate was evaporated to dryness. Column chromatographic purification of the resulting residue using silica gel (60–120 mesh size) and 4% (v/v) methanol-chloroform as eluent afforded 3.75 g (58.5%) of the title compound as a white solid (R_f = 0.35, 10% methanol/ chloroform, v/v).

N-n-tetradecyl-3,4-dihydroxypyrrolidine (II, R_1 = n-$C_{14}H_{29}$, Figure 1A). ^{1}H NMR (200 MHz, $CDCl_3$): δ/ppm = 0.90 [t, 3H, $C\underline{H}_3$-$(CH_2)_{13}$-], 1.10-1.35 [bs, 22H, -$(C\underline{H}_2)_{11}$-], 1.40-1.50 [m, 2H, N(-CH_2-$C\underline{H}_2$-)], 2.30-2.55 [m, 4H, N-$C\underline{H}_2$-$(CH_2)_{11}$, $\underline{H}_a\underline{H}_b$C(CHOH)-$NR_1$-C(CHOH)$\underline{H}_a\underline{H}_b$]; 2.85-3.00 [m, 2H, $\underline{H}_a\underline{H}_b$C(CHOH)-$NR_1$-(CHOH)$CH_a\underline{H}_b$], 4.00-4.15 [bs, 2H, -C<u>H</u>(OH)-C<u>H</u>(OH)-], 4.80-5.00 [bs, 2H, OH]. FABMS (LSIMS): m/z: 300 $[M+1]^+$ for $C_{18}H_{37}O_2N$.

N-n-hexadecyl-3,4-dihydroxypyrrolidine (II, R_1 = n-$C_{16}H_{33}$, Figure 1A). ^{1}H NMR (200 MHz, $CDCl_3$): δ/ppm = 0.90 [t, 3H, $C\underline{H}_3$-$(CH_2)_{15}$-], 1.15-1.35 [bs, 26H, -$(C\underline{H}_2)_{13}$-], 1.40-1.50 [m, 2H, N(-CH_2-$C\underline{H}_2$-)], 2.30-2.50 [m, 4H, N-$C\underline{H}_2$-$(CH_2)_{14}$, $\underline{H}_a\underline{H}_b$C(CHOH)-$NR_1$-C(CHOH)$\underline{H}_a\underline{H}_b$], 2.85-3.00[m, 2H, $\underline{H}_a\underline{H}_b$C(CHOH)-$NR_1$-(CHOH)$CH_a\underline{H}_b$], 4.00-4.15 [bs, 2H, -C<u>H</u>(OH)-C<u>H</u>(OH)-], 3.4 [s, 2H, O<u>H</u>].

N-n-octadecyl-3,4-dihydroxypyrrolidine (II, R_1 = n-$C_{18}H_{37}$, Figure 1A). ^{1}H NMR (200 MHz, $CDCl_3$): δ/ppm = 0.90 [t, 3H, $C\underline{H}_3$-$(CH_2)_{17}$-], 1.10-1.35 [bs, 30H, -$(C\underline{H}_2)_{15}$-], 1.40-1.50 [m, 2H, N(-CH_2-$C\underline{H}_2$-)], 2.30-2.55 [m, 4H, N-$C\underline{H}_2$-$(CH_2)_{16}$, $\underline{H}_a\underline{H}_b$C(CHOH)-$NR_1$-C(CHOH)$\underline{H}_a\underline{H}_b$], 2.85-3.00 [m, 2H, $\underline{H}_a\underline{H}_b$C(CHOH)-$NR_1$-(CHOH)$CH_a\underline{H}_b$]; 4.0-4.15 [bs, 2H, -C<u>H</u>(OH)-C<u>H</u>(OH)-], 1.80-2.20 [bs, 2H, O<u>H</u>]. FABMS (LSIMS): m/z: 356 $[M+1]^+$ for $C_{22}H_{45}O_2N$.

Step C

Synthesis of N,N-di-n-tetradecyl-3,4-dihydroxy pyrrolidinium chloride (R_1 = R_2 = n-$C_{14}H_{29}$, Figure 1A). N-n-tetradecyl-3,4-dihydroxy-pyrrolidine **II**, (1g, 3.3 mmole, prepared in Step B above) and n-tetradecylbromide (3 ml, 10.0 mmol) were dissolved in ethylacetate:acetonitrile solvent mixture (3:1, 40 ml) in a 100 ml round-bottomed flask and refluxed for 96 hr. The solvent was evaporated on a rotary evaporator, and column chromatographic purification of the residue (using 60–120 mesh silica gel and 4% methanol-chloroform, v/v, as eluent) followed by chloride ion exchange in Amberlyst A-26 using methanol as the eluent afforded the title compound as a white solid (1.17 g, 66%, R_f = 0.3, 10% methanol/chloroform, v/v).

N,N-di-n-tetradecyl-3,4-dihydroxy pyrrolidinium chloride, Lipid 1 (R_1 = R_2 = n-$C_{14}H_{29}$, Figure 1A). ^{1}H NMR (200 MHz, $CDCl_3$): δ/ppm = 0.90 [t, 6H, $C\underline{H}_3$- $(CH_2)_{13}$-], 1.20-1.40 [bs, 44H, -$(C\underline{H}_2)_{11}$-], 1.50-1.80 [m, 4H, N(-CH_2-$C\underline{H}_2$-)$_2$], 3.40-3.50 [t, 4H, N $(C\underline{H}_2$-$(CH_2)_{12}$], 3.70-4.00 [m, 4H, $\underline{H}_2$C(CHOH)-$N^+R_1R_2$-(CHOH)$C\underline{H}_2$], 4.50-4.60 [bs, 2H, -C<u>H</u>(OH)-C<u>H</u>(OH)-], 6.00-6.10 [bs, 2H, -O<u>H</u>]. FABMS (LSIMS): m/z: 496 $[M]^+$ for $C_{32}H_{66}O_2N$.

N,N-di-n-hexadecyl-3,4-dihydroxypyrrolidinium chloride, Lipid 2 (R_1 = R_2 = n-$C_{16}H_{33}$, Figure 1A). ^{1}H NMR (200 MHz, $CDCl_3$): δ/ppm = 0.90 [t, 6H, $C\underline{H}_3$- $(CH_2)_{15}$-], 1.20-1.40 [bs, 52H, -$(C\underline{H}_2)_{13}$-], 1.60-1.90 [m, 4H, N(-CH_2-$C\underline{H}_2$-)$_2$], 3.30-3.50 [bs, 4H, N $C\underline{H}_2$-$(CH_2)_{14}$-], 3.70-4.00 [m, 4H, $\underline{H}_2$C(CHOH)-$N^+R_1R_2$-(CHOH)$C\underline{H}_2$], 4.50-4.60 [bs, 2H, -C<u>H</u>(OH)-C<u>H</u>(OH)-], 6.00-6.20 [bs, 2H, -O<u>H</u>]. FABMS (LSIMS): m/z: 552 $[M]^+$ for $C_{36}H_{74}O_2N$.

N,N-di-n-octadecyl-3,4-dihydroxy pyrrolidinium chloride, Lipid 3 (R_1 = R_2 = n-$C_{18}H_{37}$, Figure 1A). ^{1}H NMR (200 MHz, $CDCl_3$): δ/ppm = 0.90 [t, 6H, $C\underline{H}_3$- $(CH_2)_{17}$-], 1.20-1.40 [bs, 60H, -$(C\underline{H}_2)_{15}$-], 1.50-1.80 [m, 4H, N(-CH_2-$C\underline{H}_2$-)$_2$], 3.40-3.50 [t, 4H, N-$C\underline{H}_2$-$(CH_2)_{16}$-], 3.70-4.00 [m, 4H, $\underline{H}_2$C(CHOH)-$N^+R_1R_2$-(CHOH)$C\underline{H}_2$], 4.50-4.60 [bs, -C<u>H</u>(OH)-C<u>H</u>(OH)-], 6.00-6.10 [bs, 2H, -O<u>H</u>]. FABMS (LSIMS): m/z: 608 $[M]^+$ for $C_{40}H_{82}O_2N$.

N-n-octadecyl-N-oleyl-3,4-dihydroxy pyrrolidinium chloride, Lipid 4 (R_1 = n-$C_{18}H_{37}$, R_2= oleyl, Figure 1A). ^{1}H NMR (200 MHz, $CDCl_3$): δ/ppm = 0.90 [t, 6H, $C\underline{H}_3$-$(CH_2)_{17}$-], 1.20-1.45 [bs, 54H, -$(C\underline{H}_2)_{27}$-], 1.60-1.80 [m, 4H, N(-CH_2-$C\underline{H}_2$-)$_2$], 1.90-2.20[m, 4H, -$C\underline{H}_2$-CH=CH-$C\underline{H}_2$-], 3.35-3.50 [bs, 4H, N-$C\underline{H}_2$-$(CH_2)_{16}$-], 3.70-4.00 [m, 4H, $\underline{H}_2$C(CHOH)-$N^+R_1R_2$-(CHOH)$C\underline{H}_2$], 4.60 [bs, 2H, -C<u>H</u>(OH)-C<u>H</u>(OH)-], 5.30 [t, 2H, -CH_2-C<u>H</u>=C<u>H</u>-CH2-], 6.00-6.20 [bs, 2H, -O<u>H</u>]. FABMS (LSIMS): m/z: 607 $[M+1]^+$ for $C_{40}H_{80}O_2N$.

Animals and Cells

Male Balb/c mice were obtained from National Institute of Nutrition, Hyderabad, India, and all of the in vivo experiments were performed

in accordance with the Institutional Bio-Safety and Ethical Committee guidelines using an approved animal protocol. COS-1 (SV 40 transformed African green monkey kidney cells), CHO (Chinese hamster ovary), and HepG2 (Human hepatocarcinoma) cell lines were procured from the National Centre for Cell Sciences (NCCS), Pune, India. Cells were cultured at 37°C in Dulbecco's modified Eagle's medium (DMEM) with 10% Fetal Bovine serum, 50 μg/ml penicillin, 50 μg/ml streptomycin, and 20 μg/ml kanamycin in a humidified atmosphere containing 5% CO_2.

Plasmids

pCMV-Luc and pCMV-SPORT-β-gal plasmids were generous gifts from Dr. Leaf Huang (Department of Pharmacogenetics, University of Pittsburgh, School of Medicine, Pittsburgh, PA) and Dr. Nalam Madhusudhana Rao (Centre for Cellular and Molecular Biology, Hyderabad, India), respectively. These plasmids were amplified in the DH5α strain of *Escherichia coli*, isolated by alkaline lysis procedure, and finally purified by PEG-8000 precipitation as described previously [36]. The purity of plasmid was checked by A_{260}/A_{280} ratio (around 1.9) and 1% agarose gel electrophoresis.

Preparation of Liposomes and Lipid-DNA Complexes

Cationic lipids and cholesterol (in 1:1 molar ratio) in chloroform were taken in 30 ml glass culture tubes, dried under a stream of nitrogen gas, and vacuum dessicated for a minimum of 6 hr to remove any residual organic solvent. The dried lipid film was hydrated in sterile deionized water (for in vitro) or 5% w/v glucose water (for in vivo) in a total volume of 5 ml at cationic lipid concentration of 1 mM and 5 mM, respectively, for a minimum of 12 hr. Liposomes were vortexed for 2–3 min to remove any adhering lipid film and sonicated in a bath sonicator (ULTRAsonik 28X) for 2–3 min at room temperature to produce multilamellar vesicles (MLV). MLVs were then sonicated with a Ti-probe (using a Branson 450 sonifier at 100% duty cycle and 25 W output power) in an ice bath for 1–2 min to produce small unilamellar vesicles (SUVs) as indicated by the formation of a clear translucent solution. For preparation of lipid-DNA complexes (in vivo), pDNA (25 μg) and cationic liposomes (using appropriate volumes of stock liposomes and pDNA for preparing lipoplexes with the lipid:DNA molar ratio of 4:1) were diluted to 150 μl each with 5% w/v glucose solution in sterile 1.5 ml microfuge tubes separately. The pDNA solution was added to the liposomes, mixed properly by pipetting up and down a few times, and kept at room temperature for 15–30 min before use. The final concentration of pDNA and cationic lipids (**1–8**) used for intravenous injection were 83.3 μg/ml and 536–650 μg/ml, respectively.

In Vivo Delivery and Gene Expression

Each 6-week-old male Balb/c mouse (~20 g) was injected in the tail vein with 300 μl of the liposome-DNA complexes using a 26.5 gauge syringe needle. Mice were sacrificed 8 hr post-injection, and organs were harvested and washed in cold saline. Four hundred microliters of lysis buffer (0.1 M Tris-HCl, 2 mM EDTA, and 0.2% Triton X-100, pH 7.8) was added to each organ and homogenized using a mechanical homogenizer. The homogenates were centrifuged at 14,000 rpm for 10 min at 4°C, and 2–5 μl of the supernatant was assayed using the Promega Luciferase assay kit (Madison, WI) in a Microplate Luminometer (Berthold, Germany). Protein concentration of each tissue extract was determined by the modified Lowry procedure [37], and the luciferase activity in each organ was expressed as the relative light unit (RLU) per mg of extracted protein.

In Vitro Transfection Studies

Cells were seeded at a density of 15,000 (for COS-1) and 20,000 (for CHO and HepG2) per well in a 96-well plate 18–24 hr before transfection. 0.30 μg of pDNA was complexed with varying amounts of lipids (to give +/− ratios of 0.1:1, 0.3:1, 1:1, 3:1, and 9:1) in plain DMEM (total volume made up to 100 μl) for 20–30 min. The complexes were then added to the cells. After 3 hr of incubation, 100 μl of DMEM with 20% FBS was added to the cells. The medium was changed to complete medium containing 10% FBS after 24 hr, and the reporter gene activity was estimated after 48 hr. Cells were washed with PBS (100 μl) and lysed in 50 μl lysis buffer (0.25 M Tris-HCl [pH 8.0], 0.5% NP40). The β-galactosidase activity per well was estimated by adding 50 μl of 2X-substrate solution (1.33 mg/ml *o*-nitrophenyl-β−D-galactopyranoside, 0.2 M sodium phosphate [pH 7.3], and 2 mM magnesium chloride) to the lysate in a 96-well plate. Absorbance of the product ortho-nitrophenol at 405 nm was converted to β-galactosidase units by using a calibration curve constructed using pure commercial β-galactosidase enzyme. The transfection values reported are the average values from two replicate experiments performed in the same plate on the same day. Each transfection experiment was performed three times on three different days. The day-to-day variation in transfection efficiency was mostly within 2- to 3-fold and was dependent on the cell density and condition of the cells.

Zeta Potential and Size Measurments

The sizes and the global surface charges (zeta potentials) of lipoplexes were measured by photon correlation spectroscopy and electrophoretic mobility with a Zetasizer 3000HSA (Malvern Instruments, United Kingdom). The system was calibrated by using the 199 ± 6 nm Nanosphere Size Standard (Duke Scientific Corp., Palo Alto, CA) and DTS 0050 standard from Malvern.

DNA Binding Assay

The DNA binding ability of cationic lipids **1–7** was assessed by their gel retardation assay on a 1% agarose gel. 0.30 μg of pCMV-Luc was complexed with the cationic lipids (at a cationic lipid:DNA molar ratio of 4:1) in a total volume of 16 μl in HEPES buffer (pH 7.40) and incubated at room temperature for 20–25 min. Three micoliters of 6X loading buffer (0.25% bromo phenol blue, 40% sucrose) was added to it, and 6.3 μl of the resultant solution was loaded on each well. The samples were electrophoresed at 80 V for approximately 2 hr, and the DNA bands were visualized by staining overnight with ethidium bromide solution.

DNase 1 Sensitivity Assay

Briefly, in a typical assay 1.5 nmol of DNA (500 ng) was complexed with lipid using the indicated lipid:DNA charge ratios (Figure 5B), and the mixture was incubated at room temperature for 30 min on a rotary shaker. Subsequently, the complexes were treated with DNase I (at a final concentration of 5 ng/1.5 nmol of pDNA) in the presence of 20 mM $MgCl_2$. The volume was made up to 50 μl with 10 mM HEPES buffer (pH 7.4) and incubated for 20 min at 37°C. The reactions were then halted by adding EDTA (to a final concentration of 20 mM) and incubated at 60°C for 10 min in a water bath. The aqueous layer was washed with 50 μl of phenol:chloroform mixture (1:1, v/v) and centrifuged at 10,000 rpm at 4°C for 5 min. The aqueous supernatant was separated, loaded (20 μl) on a 1% agarose gel, and electrophoresed at 90 V for 3 hr. The bands were visualized with ethidium bromide staining.

Toxicity Assay

Cytotoxicities of lipids **1–8** were assessed by the 3-(4,5-dimethylthiazol-2-yl)-2,5-diphenyltetrazolium bromide (MTT) reduction assay as described earlier [38]. The cytotoxicity assay was performed in 96-well plates using the same conditions as described for the transfection experiments. Briefly, after 3 hr of lipid:DNA complex addition, DMEM containing 20% FBS (100 μl) and MTT (10 μl, 5 mg/ml in PBS buffer) was added to each well. After 3–4 hr, medium was removed, 100 μl of DMSO:Methanol (1:1, v/v) was added to each well and shaken in a rotary shaker for 20–25 min. Results are expressed as percent viability = $[A_{550}$(treated cells)-background/A_{550}(untreated cells)-background$] \times 100$.

Transmission Electron Microscopy

Electron microscopy was performed on a FEI Tecnai 12 TEM apparatus operated at 100 KV. Lipoplex samples were transferred onto an ultrathin-carbon-coated copper grid by placing the grid on top of a 10 μl drop of the sample for 1 min. After wicking away the excess fluid from one side, the grid was placed on a 100 μl water drop for 30 s wash. The excess fluid was removed and the grid was placed for 1 min on a 20 μl drop of freshly filtered uranyl acetate (1.33%). Once again, the excess fluid was wicked away and the grid was air dried.

Acknowledgments

Financial support (to A.C.) from the Department of Biotechnology, Government of India, New Delhi, is gratefully acknowledged. Financial support from the Council of Scientific and Industrial Research (CSIR), Government of India (to B.K.M., R.S.S., and S.K.Y.) and University Grants Commision (UGC), Government of India (to S.R.B.) is also gratefully acknowledged. Raghavendra Reddy and Sudhakar are sincerely thanked for helping with the in vivo experiments. Nisha is also thanked for help in procuring gel pictures. This is IICT Communication No. 030802.

Received: September 12, 2003
Revised: December 6, 2003
Accepted: January 5, 2004
Published: April 16, 2004

References

1. Verma, I.M., and Somina, M. (1997). Gene therapy-promises, problems and prospects. Nature *389*, 239–242.
2. Anderson, W.F. (1998). Human gene therapy. Nature *392*, 25–30.
3. Yla-Herttuala, S., and Martin, J.F. (2000). Cardiovascular gene therapy. Lancet *355*, 213–222.
4. Yang, Y., Nunes, F.A., Berencsi, K., Furth, E.E., Gonczol, E., and Wilson, J.M. (1994). Cellular immunity to viral antigens limits E1-deleted adenoviruses for gene therapy. Proc. Natl. Acad. Sci. USA *91*, 4407–4411.
5. Knowles, M.R., Hohneker, K.W., Zhou, Z., Olsen, J.C., Noah, T.L., Hu, P.C., Leigh, M.W., Engelhardt, J.F., Edwards, L.J., Jones, K.R., et al. (1995). A controlled study of adenoviral-vector-mediated gene transfer in the nasal epithelium of patients with cystic fibrosis. N. Engl. J. Med. *333*, 823–831.
6. Crystal, R.G., McElvaney, N.G., Rosenfeld, M.A., Chu, C.S., Mastrangeli, A., Hay, J.G., Brody, S.L., Jaffe, H.A., Eissa, N.T., and Danel, C. (1994). Administration of an adenovirus containing the human CFTR cDNA to the respiratory tract of individuals with cystic fibrosis. Nat. Genet. *8*, 42–51.
7. Yang, Y., Nunes, F.A., Berencsi, K., Gonczol, E., Engelhardt, J.F., and Wilson, J.M. (1994). Inactivation of E2a in recombinant adenoviruses improves the prospect for gene therapy in cystic fibrosis. Nat. Genet. *7*, 362–369.
8. Lehrman, S. (1999). Virus treatment questioned after gene therapy death. Nature *401*, 517–518.
9. Fox, J.L. (1999). Gene therapy safety issues come to fore. Nat. Biotechnol. *17*, 1153.
10. Liu, Y., Mounkes, L.C., Liggit, H.D., Brown, C.S., Solodin, I., Heath, T.D., and Debs, R.J. (1997). Factors influencing the efficiency of cationic liposome-mediated intravenous gene delivery. Nat. Biotechnol. *15*, 167–173.
11. Templeton, N.S., Lasic, D.D., Frederik, P.M., Strey, H.H., Roberts, D.D., and Pavlakis, G.N. (1997). Improved DNA:liposome complexes for increased systemic delivery and gene expression. Nat. Biotechnol. *15*, 647–652.
12. Zhu, N., Liggit, D., Liu, Y., and Debs, R. (1993). Systemic gene expression after intravenous DNA delivery in adult mice. Science *261*, 209–211.
13. Hara, T., Tan, Y., and Huang, L. (1997). In vivo gene delivery to the liver using reconstituted chylomicron remnants as a novel non-viral vector. Proc. Natl. Acad. Sci. USA *94*, 14547–14552.
14. Putnam, D., Gentry, C.A., Pack, D.W., and Langer, R. (2001). Polymer-based gene delivery with low cytotoxicity by a unique balance of side-chain termini. Proc. Natl. Acad. Sci. USA *98*, 1200–1205.
15. Alton, E.W., Stern, M., Farley, R., Jaffe, A., Chadwick, S.L., Phillips, J., Davies, J., Smith, S.N., Browning, J., Davies, M.G., et al. (1999). Cationic lipid-mediated *CFTR* gene transfer to the lungs and nose of patients with cystic fibrosis: a double-blind placebo-controlled trial. Lancet *353*, 947–954.
16. Oudrhiri, N., Vigneron, J.P., Peuchmaur, M., Leclerc, T., Lehn, J.M., and Lehn, P. (1997). Gene transfer by guanidinium-cholesterol cationic lipids into airway epithelium cells in vitro and in vivo. Proc. Natl. Acad. Sci. USA *94*, 1651–1656.
17. Yotnda, P., Chen, D.H., Chiu, W., Piedra, P.A., Davis, A., Templeton, N.S., and Brenner, M.K. (2002). Bilamellar cationic liposomes protect adenovectors from pre-existing humoral immune responses. Mol. Ther. *5*, 233–241.
18. Shi, H.Y., Liang, R., Templeton, N.S., and Zhang, M. (2002). Inhibition of breast tumor progression by systemic delivery of the maspin gene in a syngenic tumor model. Mol. Ther. *5*, 755–761.
19. Banerjee, R., Das, P.K., Srilakshmi, G.V., Chaudhuri, A., and Rao, N.M. (1999). A novel series of non-glycerol based cationic transfection lipids for use in liposomal gene delivery. J. Med. Chem. *42*, 4292–4299.
20. Banerjee, R., Mahidhar, Y.V., Chaudhuri, A., Gopal, V., and Rao, N.M. (2001). Design, synthesis and transfection biology of novel cationic glycolipids for use in liposomal gene delivery. J. Med. Chem. *44*, 4176–4185.
21. Vinod Kumar, V., Pichon, C., Refregiers, M., Guerin, B., Midoux, P., and Chaudhuri, A. (2003). Single histidine residue in headgroup region is sufficient to impart remarkable gene transfection properties to cationic lipids: Evidence for histidine-mediated membrane fusion at acidic pH. Gene Ther. *10*, 1206–1215.
22. Felix, R., and Doring, G. (2003). Cystic fibrosis. Lancet *361*, 681–689.
23. Lee, E.R., Marshall, J., Siegel, C.S., Jiang, C., Yew, N.S., Nichols, M.R., Nietupski, J.B., Ziegler, R.J., Lane, M.B., Wang, K.X., et al. (1996). Detailed analysis of structures and formulations of cationic lipids for efficient gene transfer to the lung. Hum. Gene Ther. *7*, 1701–1717.
24. Alton, E.W., Middleton, P.G., Caplen, N.J., Smith, S.N., Steel, D.M., Munkonge, F.M., Jeffery, P.K., Geddes, D.M., Hart, S.L., Williamson, R., et al. (1993). Non-invasive liposome-mediated gene delivery can correct the ion-transport defect in cystic fibrosis mutant mice. Nat. Genet. *5*, 135–142.
25. Alton, E.W.F.W., Geddes, D.M., Gill, D.R., Higgins, C.F., Hyde, S.C., Innes, J.A., and Porteous, D.J. (1998). Towards gene therapy for cystic fibrosis: A clinical progress report. Gene Ther. *5*, 291–292.
26. Engelhardt, J.F. (2002). The lung as a metabolic factory for gene therapy. J. Clin. Invest. *110*, 429–432.
27. Singh, R.S., Mukherjee, K., Banerjee, R., Chaudhuri, A., Hait, S.K., Moulik, S., Ramadas, Y., Vijayalakshmi, A., and Rao, N.M. (2002). Anchor dependency for non-glycerol based cationic lipofectins: Mixed bag of regular and anomalous transfection profiles. Chemistry *8*, 900–909.
28. Skarzewski, J., and Gupta, A. (1997). Synthesis of C2 symmetric primary vicinal diamines. Double stereospecific Mitsunobo reaction on the heterocyclic diols derived from tartaric acid. Tetrahedron: Asymmetry *8*, 1861–1867.
29. Sorgi, F.L., Bhattacharya, S., and Huang, L. (1997). Protamine sulfate enhances lipid-mediated gene transfer. Gene Ther. *4*, 961–968.
30. Li, S., and Huang, L. (1997). In vivo gene transfer via intravenous administration of cationic lipid-protamine-DNA (LPD) complexes. Gene Ther. *4*, 891–900.
31. Mclean, J.W., Fox, E.A., Baluk, P., Bolton, P.B., Haskell, A., Pearlman, R., Thurston, G., Umemoto, E.Y., and McDonald, D.M. (1997). Organ-specific endothelial cell uptake of cationic liposome-DNA complexes in mice. Am. J. Physiol. Heart Circ. Physiol. *273*, H387–H404.
32. Uyechi, L.S., Gagne, L., Thurston, G., and Szoka, F.C., Jr. (2001). Mechanism of lipoplex gene delivery in mouse lung: binding and internalization of fluorescent lipid and DNA components. Gene Ther. *8*, 828–836.
33. Li, S., Tseng, W.C., Stolz, D.B., Wu, S.P., Watkins, S.C., and Huang, L. (1999). Dynamic changes in the characteristics of cationic lipidic vectors after exposure to mouse serum: Implications for intravenous lipofection. Gene Ther. *6*, 585–594.
34. Tandia, B.M., Vanderbranden, M., Wattiez, R., Lakhdar, Z., Ruysschaert, J.M., and Elouahabi, A. (2003). Identification of human plasma proteins that bind to cationic lipid/DNA complex and analysis of their effects on transfection efficiency: Implications for intravenous gene transfer. Mol. Ther. *8*, 264–273.
35. Son, K.K., Tkach, D., and Patel, D.H. (2000). Zeta potential of transfection complexes formed in serum-free medium can pre-

dict in vitro gene transfer efficiency of transfection reagent. Biochim. Biophys. Acta *1468*, 11–14.
36. Sambrook, J., and Russell, D.W. (2001). Molecular Cloning: A Laboratory Manual, Third Edition (Cold Spring Harbor, NY: Cold Spring Harbor Laboratory Press).
37. Markwell, M.A., Haas, S.M., Bieber, L.L., and Tolbert, N.E. (1978). A modification of the Lowry procedure to simplify protein determination in membrane and lipoprotein samples. Anal. Biochem. *87*, 206–210.
38. Hansen, M.-B., Neilson, S.E., and Berg, K. (1989). Re-examination and further development of a precise and rapid dye method for measuring cell growth/cell kill. J. Immunol. Methods *119*, 203–210.